Supporting Information

Role of Delamination in Zeolite-Catalyzed Aromatic Alkylation: UCB-3 versus 3-D Al-SSZ-70

Ron C. Runnebaum[1], Xiaoying Ouyang[1], Jeffrey A. Edsinga[1], Thomas Rea[4], Ilke Arslan[2], Son-Jong Hwang[3], Stacey I. Zones[,1,4], Alexander Katz[*,1]*

[1]Department of Chemical and Biomolecuar Engineering, University of California, Berkeley, CA 94720, USA.

[2]Pacific Northwest National Laboratory, Richland, WA 99352 USA

[3]Division of Chemistry and Chemical Engineering, California Institute of Technology, Pasadena, CA 91125, USA.

[4]Chevron Energy Technology Company, Richmond, CA 94804, USA

[*]E-mail addresses: askatz@berkeley.edu (A.K.), sizo@chevron.com (S.I.Z.).

Table of Contents:

1 Experimental

1.1 Materials and sample preparation

All reagents used in zeolite synthesis, delamination, and chemisorption were of reagent-grade quality and were used as received.

1.1.1 Preparation of 1,3-Diisobutylimidazolium Hydroxide (SDA) Solution.

Synthesis of 1,3-diisobutylimidazolium bromide (SDA^+Br^-) was performed according to previously described literature.[1] SDA^+Br^- was ion-exchanged to the hydroxide form by contacting with two equivalents of an ion-exchange resin (Bio-Rad, AG1-X8) in water at room temperature for 24 h.

1.1.2 Synthesis of Al-SSZ-70.

Synthesis of Al-SSZ-70 (Si/Al = 40) was performed according to previously described literature.[1] Typically, 0.171 g of aluminum hydroxide (Reheis F-2000, 50-53 wt% Al_2O_3) was dissolved in a mixture of 8.89 g of 1 N sodium hydroxide aqueous solution (Sigma-Aldrich), 6.88 g of distilled water, and 35.6 g of 0.5 mmol/g of SDA^+OH^- solution. To this mixture, 5.5 g of fumed silica (Sigma-Aldrich, particle size, 0.007 μm) and seed crystals (as-made Al-SSZ-70, 1% of SiO_2) were added. The gel composition was SiO_2 : 0.010 Al_2O_3 : 0.050 Na_2O : 0.20 SDA : 30 H_2O. After the gel was stirred at room temperature overnight, it was divided into four portions, and each gel was transferred to a 23-mL Parr reactor equipped with a Teflon liner. Each reactor was sealed and heated while tumbling at 60 rpm at 423 K for a period of 1–2 weeks. After cooling, the solid product was collected by centrifugation, washed thoroughly with distilled water, and dried at 353 K in a convection oven overnight. Calcination of Al-SSZ-70 was performed in an O_2/Ar flow at 823 K for 12 h. The product was determined by X-ray diffraction (XRD) to be SSZ-70.

1.1.3 Synthesis of UCB-3 via Delamination of Al-SSZ-70.

Synthesis of UCB-3 (Si/Al = 40) was performed according to previously described literature.[2] A mixture of 0.50 g of as-made Al-SSZ-70 , 0.55 g of cetyltrimethylammonium bromide (CTAB) (Sigma-Aldrich, ≥99.0%), 0.85 g of tetrabutylammonium fluoride trihydrate (TBAF) (Sigma-Aldrich, ≥97%), and 0.85 g of tetrabutylammonium chloride (TBACl) (Sigma-Aldrich, ≥97%) in 20 mL of DMF (Fischer Scientific) was placed in a screw-capped 50 mL PFA tube, and stirred using a magnetic stir bar at 373 K for 16 h in an oil bath. After cooling, the slurry was sonicated for 1 h in an ice bath, using a Branson digital sonifier 450 (Branson, USA) operating under pulse mode (1.0 s on and 0.1 s off). The sonicated slurry was filtered so as to separate a solid from a brown-colored filtrate. The solid was washed with DMF and then with ethanol thoroughly, and dried at 323 K overnight, yielding a white solid. Calcination of UCB–3 was performed in an O_2/Ar flow at 823 K for 12 h.

1.1.4 Ion-exchange of Al-SSZ-70 or UCB-3.

Calcined material was contacted with 0.2 M NH_4NO_3 aq. (NH_4^+/Al ratio > 10) at 353 K for 1 h. This procedure is repeated four times, and the slurry was filtered. The resultant solid was dried at 353 K in a convection oven overnight. The ammonium–exchanged material was calcined to the H-form zeolite under the following conditions: under flowing dry air, the temperature was increased to 823 K at a rate of 1 K min^{-1} and soaked at this temperature for 5 h.

1.1.5. *Silica-modification of H-Al-SSZ-70 external acid sites.*

Synthesis of a silica-modified zeolite, to cap the external acidic hydroxyls with SiOx species lacking acidic hydroxyls, was performed according to previously described literature.[3] Silanated H–Al-SSZ-70 was prepared by stirring a slurry of H-Al-SSZ-70 (Si/Al = 25; 0.1 g) in an ethanol solution (2 mL) containing 0.03 g of 3-aminopropyl-triethoxylsilane (Aldrich, 99.9%) for 30 min. The ethanol solvent was subsequently evaporated at 333-393 K to leave the organosilane, which has a boiling point of 490 K, on the surface of the zeolite. The sample was then calcined in dry air at 823 K for 16 h (100 mL /min) to form the silanated H–Al-SSZ-70. Both the H-Al-SSZ-70 and the silanated H-Al-SSZ-70 were further characterized and used as solid acid catalysts.

1.2 Characterization

1.2.1 Amine chemisorption

Pyridine (Sigma Aldrich, spectroscopic grade) and collidine (Sigma Aldrich, 99% 2,4,6-trimethylpyridine) chemisorption experiments were performed by thermogravimetric analysis (TA Instruments TGA 2950). Approximately 30 mg of sample in the proton form was heated to 823 K in 100 mL/min of a dry N_2 flow, followed by a soak at this temperature for 3 h. After cooling to 423 K, approximately 50 μL of pyridine was injected to the inlet line via syringe, and the system remained at 423 K for 3000 min.

Acridine chemisorption experiments were performed on a Varian Cary 400 UV-VIS spectrometer. The zeolite sample was heated for at least 4 h at 448 K to remove water from the sample and cooled down in a desiccator. Acridine (Sigma Aldrich, 97%) was recrystallized two times in ethanol and used to prepare a 500 μmol acridine/g hexane stock solution. 2 mL of the acridine stock solution was added to approximately 3.00 mg zeolite for titration. In these samples, these amounts of zeolite and acridine corresponded to a 1:3 ratio of potential acid sites to mol acridine in solution. The titrated solution was collected 1 h after the titration and passed through a 0.45 μm syringe filter. The difference of UV-vis absorbance of the stock solution and titrated solution was recorded and calculated by a UV-vis spectrometer. The decrease in UV-vis absorbance after titration was used to calculate the external acid sites. Each sample was characterized three times and the measurement error is less than 5%.

1.2.2 Elemental analysis

Elemental analysis was performed at Galbraith Laboratories (Knoxville, TN). Aluminum content was determined by Inductively Coupled Plasma–Atomic Emission Spectroscopy (ICP–AES). Silicon content was determined by Flame Atomic Absorption Spectrophotometry (FLAA).

1.2.3 Powder X-ray diffraction

Powder X-ray diffraction (XRD) patterns were collected on a Bruker D8 Advance diffractometer using a Cu Kα radiation.

1.2.4 N_2 physisorption

N_2 physisorption isotherms were measured on a Micromeritics ASAP2020 at 77 K. Prior to measurement, samples were evacuated at 623 K for 4 h.

1.2.5 Scanning Electron Microscopy (SEM)

The SEM images were acquired using a JEOL JSM- 6700F instrument. In cases where delaminated UCB-3 and Al-SSZ-70 were prepared from different synthesis liners, SEM characterization was performed to ensure the same morphology at the layered zeolite precursor stage.

1.2.6. Transmission Electron Microscopy (TEM)

The TEM images were recorded on a JEOL Model JEM- 2010 (200 kV) at the University of California, Davis.

1.2.7 Scanning Transmission Electron Microscopy (STEM)

The STEM images of the zeolites were acquired on a 200kV FEI Tecnai instrument at the Pacific Northwest National Laboratory. The samples were gently crushed between glass slides and dry-loaded onto holey-carbon copper grids for both sets of experiments.

1.2.8 Solid-state nuclear magnetic resonance (NMR) measurements

^{29}Si solid-state MAS NMR spectra were measured using a Bruker Avance 500 MHz spectrometer with a wide bore 11.7 T magnet and employing a Bruker 4 mm MAS probe. The spectral frequencies were 500.23 MHz for the ^{1}H nucleus and 99.4 MHz for the ^{29}Si nucleus. ^{29}Si MAS NMR spectra were acquired after a 4 μs-90 degree pulse with application of a strong ^{1}H decoupling pulse. The spinning rate was 12 kHz, and the recycle delay time was 300 s. ^{29}Si CP MAS NMR spectra were collected at a sample spinning rate of 8 kHz, and the cross polarization contact time was 2.0 ms under the same radiofrequency pulse power (62.5 kHz ± 8 kHz). NMR shifts were reported in parts per million (ppm) when externally referenced to tetramethylsilane (TMS). One dimensional (1D) ^{27}Al MAS NMR spectra were also recorded on a Bruker DSX-500 spectrometer (130 MHz for ^{27}Al) after a 0.5 μs single pulse (nutation angle $< \pi/18$) with application of a strong

^{1}H decoupling pulse, at a sample spinning rate of 14 kHz. An external reference for ^{27}Al shift was 1 M aqueous solution of $Al(NO_3)_3$.

1.3 Alkylation of toluene with propylene catalysis

Catalytic reactions were carried out in a once-through packed-bed plug-flow reactor under the following conditions, with liquid toluene (Sigma-Aldrich, ≥99.9%) vaporized into a flowing gas stream: catalyst mass, 5-20 mg; temperature, 423–523 K; pressure, 140 kPa; toluene liquid flow rate, 0.0596 mol h^{-1}; gas feed flow rate, 0.244 mol h^{-1}, as 0.214 mol h^{-1} He (Praxair, 99.999%) and 0.0295 mol h^{-1} 20% C_3H_6 (Praxair, 5% Ar with balance He). Each catalyst powder was diluted with particles of inert, nonporous α-Al_2O_3. The product gas stream was heated to 403 K. Samples were periodically analyzed by gas chromatography.

Data were obtained using the same mass of either UCB-3 or Al-SSZ-70 under differential conversion conditions and at each temperature. Differential conversion conditions (i.e. relatively low conversion) were chosen because the rates of reaction are directly determined from the relationship of conversion as a function of space velocity,[4] and because the contributions of secondary reactions to rates of product formation are minimized. Rates of formation and selectivities for isopropyltoluene isomers and 2,4-*di*isopropyltoluene were determined. Because of the low conversion conditions, trace product FID peak areas observed were nearly two-orders of magnitude lower and were, therefore, not quantified. Differential conversion conditions have been shown for low conversion ($X < 0.2$) alkylation of aromatics by MCM–22.[5] Differential conversion conditions, used in all experiments, were achieved by changing the mass of the catalyst in the packed bed.

2 Analytical characterization of delaminated UCB-3

Several different analytical characterization techniques were used together, as has been done previously,[6] to provide strong evidence of delamination in UCB-3 materials used for catalysis here. Micrographs were obtained using scanning transmission electron microscopy, and are shown in Figure S1 (complemented by scanning electron microscopy in Figure S2). STEM images of the calcined Al-SSZ-70 in Figures S1A–C show a rectilinear morphology, whereas calcined UCB-3 in Figures S1D-F exhibits exfoliation of layers and a more curved morphology, both of which are consistent with delamination.[6,7] These images are consistent with PXRD patterns, shown in Figure S3, which also suggest a delaminated UCB-3.[1,6] Peaks, assigned to long-range order in the *c*-axis, present in precursor materials at 3.3° and 6.6° are not present in the calcined UCB-3 material. The peak at 6.6° (002) is described to shift towards the peak at 7.2° (100), which is assigned to intralayer crystallinity in MWW zeolites.[8] The resulting merged peak is retained in UCB–3 as a result of the mild delamination conditions. The 101 and 102 peaks broaden and merge into a single broad peak, indicating a less parallel alignment and stacking of the MWW-type layers.[6] Other peaks observed in Al-SSZ-70 sample are reduced or broadened as a result of exfoliation of layers, which reduces the crystalline repetition between layers, and the long-range order along the *c*-axis.[6] Additional evidence of delamination is provided by the N_2 gas physisorption isotherms in Figure S4, which show a decrease in micropore volume of UCB-3 relative to that of Al-SSZ-70. Table 1 lists the micropore and total volumes and external surface area as determined by the *t*-plot method. The delaminated material, UCB-3, shows slightly lower micropore volume and a significantly

higher external surface area. This has been previously discussed as evidence of delamination of Al-SSZ-70 precursor.[6] The changes in the TEM and physisorption are attributed to and are consistent with delamination.

^{29}Si MAS NMR spectra characterizing the calcined Al-SSZ-70 in Figure S5A and the calcined UCB-3 in Figure S5B show the complete lack of Q^2 resonance at approximately -90 ppm, which suggests a lack of amorphous silica on the zeolite framework within the actual materials used for catalysis here. This is a direct result of the mild delamination conditions. The spectra also show only slight differences between UCB-3 and Al-SSZ-70 in the Q^3 and Q^4 resonances in the range of -96.5 and -124.0 ppm. These data indicate a lack of amorphization of UCB-3 relative to Al-SSZ-70. These data are consistent with delamination of Al-SSZ-70 layers to form UCB-3 and with preserving the two-dimensional intralayer zeolite framework of UCB-3 intact because of the mild delamination conditions.[6]

To confirm the retention of Al in the zeolite framework within the actual materials used for catalysis, we examined both UCB-3 and Al-SSZ-70 by elemental analysis to determine the Si:Al ratio and characterized the Al atoms by NMR spectroscopy. The leaching of heteroatoms from the framework would lead to an increase in the Si:Al ratio. Elemental analysis data in Table 1 show no significant change in the heteroatom content of the zeolite. The Si:Al of 40 is consistent with experimental values previously reported for this Al-SSZ-70 synthesis, in which the synthesis gel contains a Si:Al of 50.[6] The ^{27}Al MAS NMR spectra characterizing calcined Al-SSZ-70 in Figure S6A and calcined UCB-3 in Figure S6B were used to confirm that the Al atoms were not leached to surface to form extra-framework Al. These spectra show the distribution over AlO_4 (50-60 ppm) and AlO_6 (0 ppm) is nearly the same for both samples. Both samples contain some octahedral Al, which is also found in calcined MWW zeolites.[9,10] Its presence does not change, however, as a result of the mild delamination conditions. These data are consistent with complete retention of Al atoms within the zeolite framework as observed previously for UCB-3.[6]

The significant increase in observed activity per gram of catalyst by UCB-3 relative to Al-SSZ-70 should reflect an increase in external surface Brønsted acid sites as a result of delamination. Total acid sites are not expected to differ dramatically and were determined by chemisorption of pyridine because it can access both the 10-MR and 12-MR channels.[11] These data are summarized in Table 1. The total acid sites were measured by first converting the Al-SSZ-70 and UCB-3 to the H-form, via NH_4^+ ion exchange followed by calcination, and then by using pyridine chemisorption at 423 K. UCB-3 showed a pyridine adsorption within 15% of Al-SSZ-70. The slightly lower uptake in pyridine observed for UCB-3 is consistent with published results,[7] and may be a result of some stacked layers aggregating after calcination and blocking access to the acid sites.

3 Supporting Information Figures

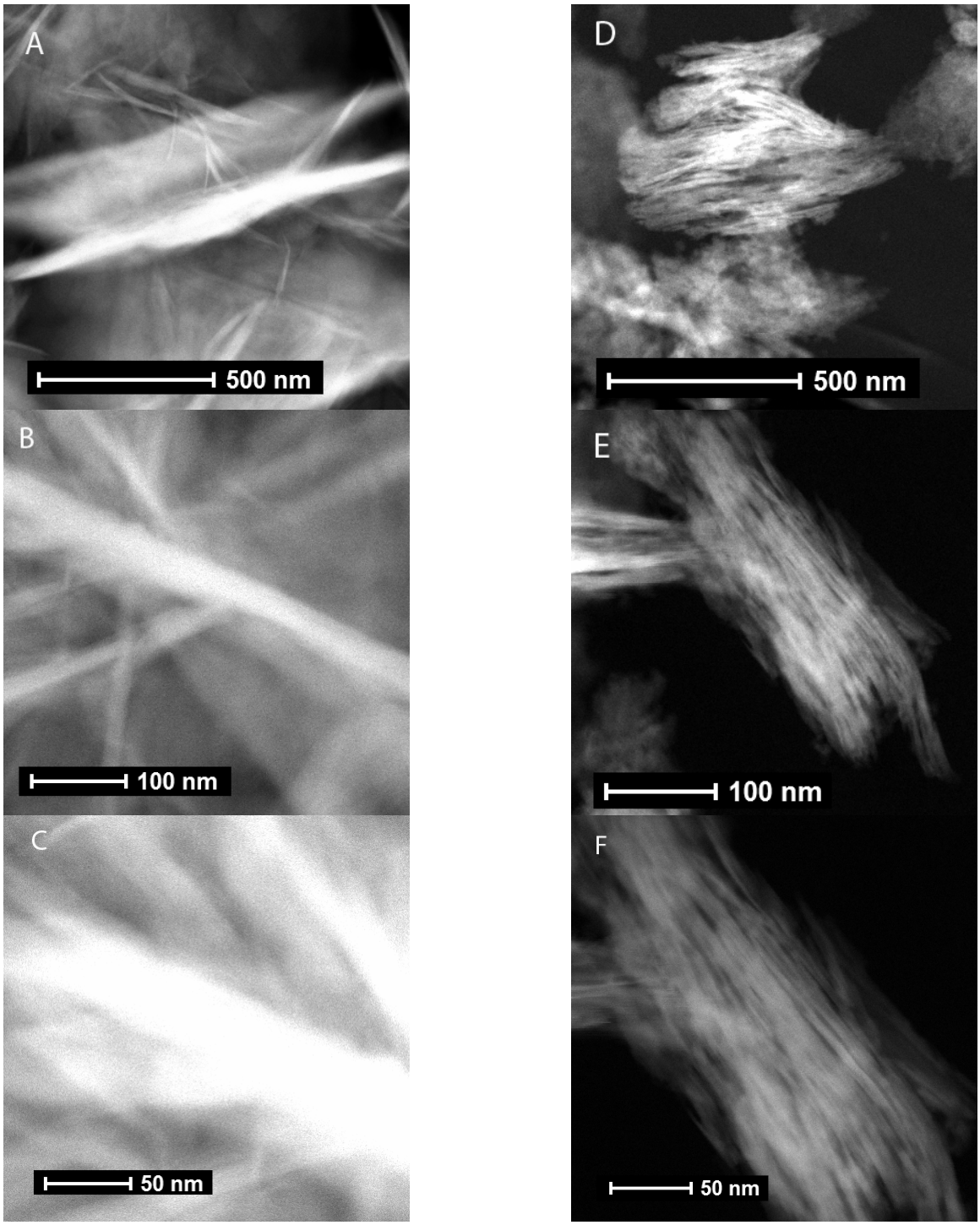

Figure S1. TEM images characterizing (A–C) Al-SSZ-70 and (D–F) UCB-3. Both materials have been calcined, ion-exchanged, and re-calcined into the H-form. The UCB-3 image show curved and exfoliated layers relative to the Al-SSZ-70 image.

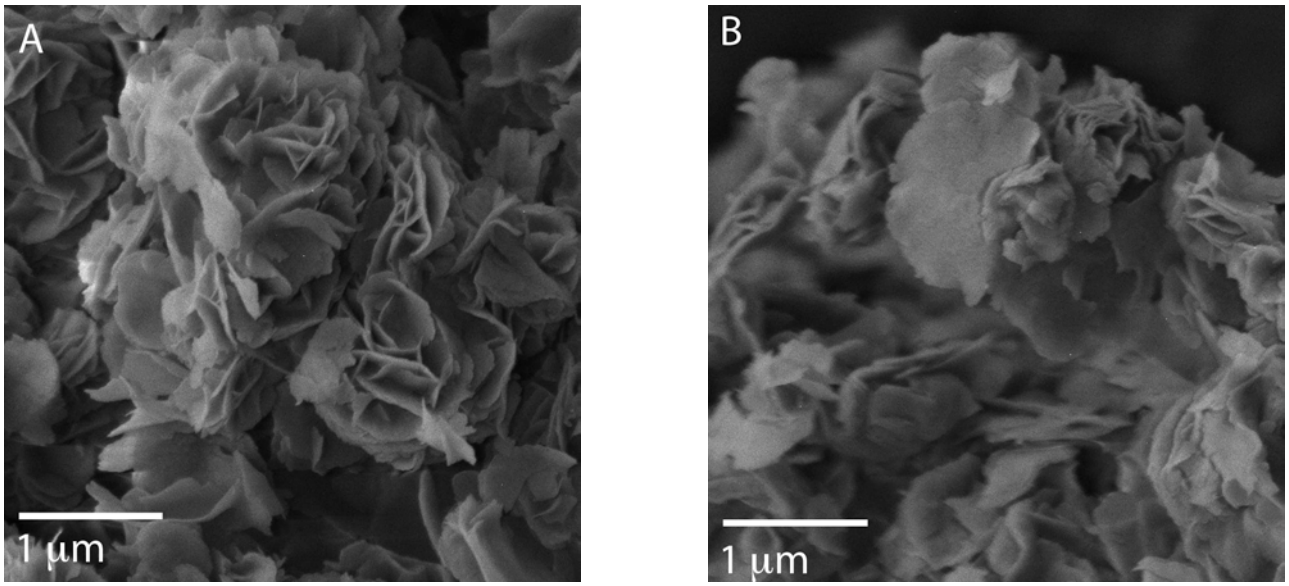

Figure S2. Scanning electron microscopy (SEM) images characterizing layered zeolite precursor materials, which were used to synthesize (A) Al-SSZ-70 and (B) UCB-3. The similar crystal size and morphology of both layered zeolite precursors in (A) and (B) point to any differences in Al-SSZ-70 and UCB-3 as not being due to the layered zeolite precursor used for their synthesis, but rather as being due to delamination procedure.

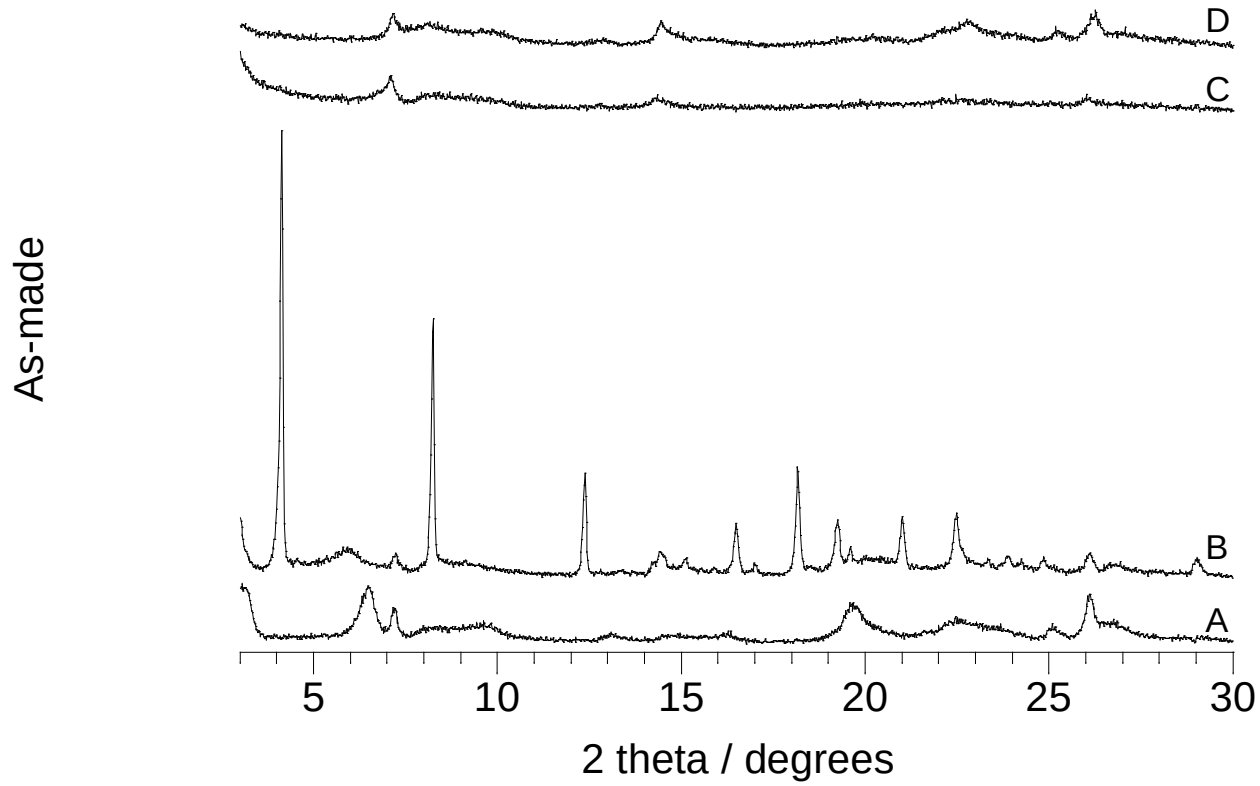

Figure S3. Powder x-ray diffraction patterns characterizing (A) as-made Al-SSZ-70, (B) swollen Al-SSZ-70, (C) calcined UCB-3 (D) calcined 3-D Al-SSZ-70. When comparing powder patterns in (A) and (B) with those that have been published previously for the same materials,[6] the loss of the peak at 6.6^{o} and the appearance of peaks at around 4^{o}, 7^{o}, and 8^{o} in pattern (B) above are characteristic of swollen Al-SSZ-70. Also, the general loss of PXRD information in powder pattern (C) is consistent with a loss of long-range order accompanying delamination.

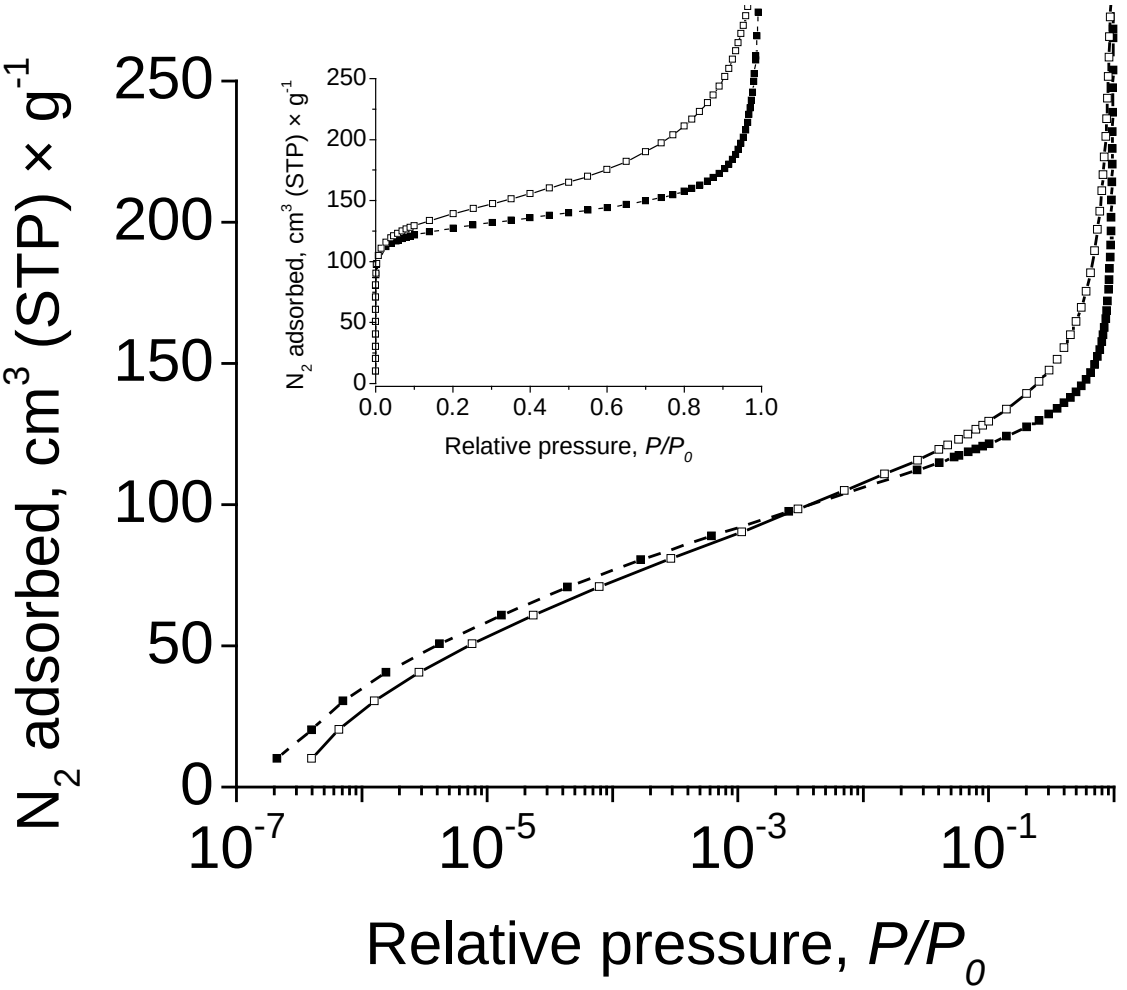

Figure S4. N_2 physisorption isotherms characterizing the following samples in a semilogarithmic scale: (■) Al-SSZ-70 and (□) UCB-3. Both materials have been calcined, ion-exchanged, and re-calcined into the H-form. The inset shows the same data in a linear scale. The isotherm shows a decrease in microporosity, which is consistent with delamination.

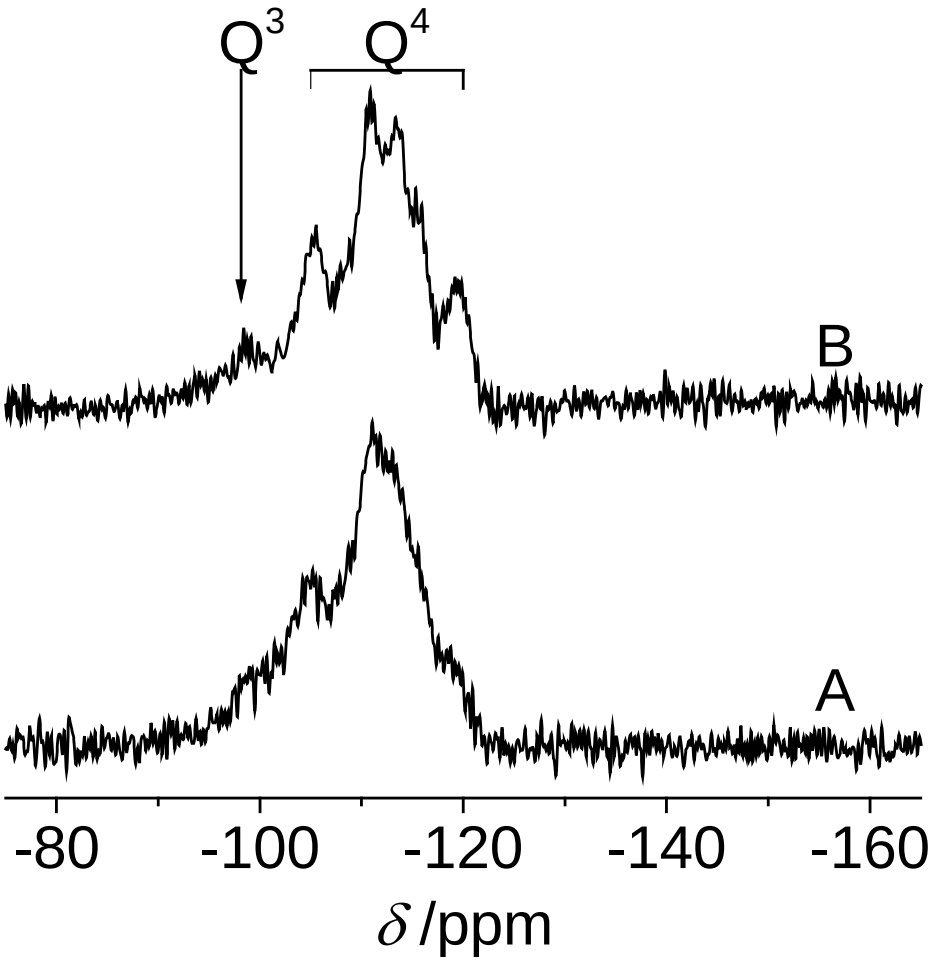

Figure S5. ^{29}Si MAS NMR spectra characterizing (A) Al-SSZ-70 (Si/Al ratio = 40) and (B) UCB-3 (Si/Al ratio = 40). Both materials have been calcined, ion-exchanged, and re-calcined into the H-form. These data indicate a lack of amorphization of UCB-3 relative to Al-SSZ-70.

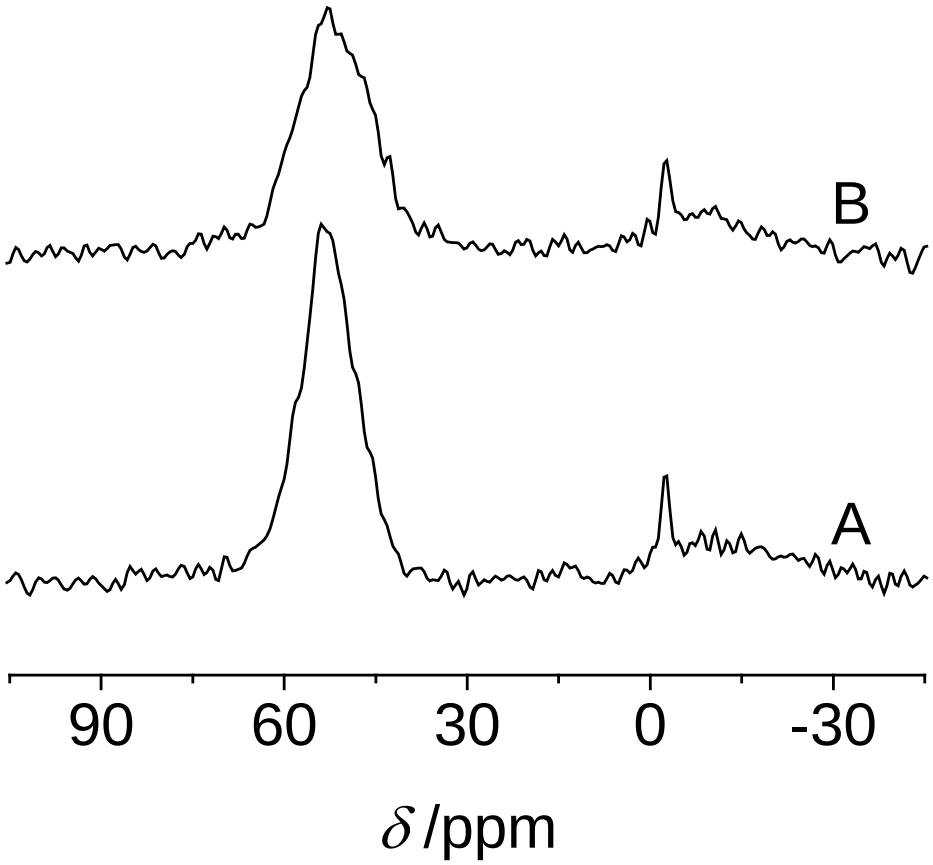

Figure S6. ^{27}Al MAS NMR spectra characterizing (A) Al-SSZ-70 (Si/Al ratio = 40) and (B) UCB-3 (Si/Al ratio = 40). Both materials have been calcined, ion-exchanged, and re-calcined into the H-form. These data show that while the AlO_4 (50-60 ppm) distribution is slightly broader for UCB-3, the distribution over AlO_4 and AlO_6 (0 ppm) is nearly the same for both samples.

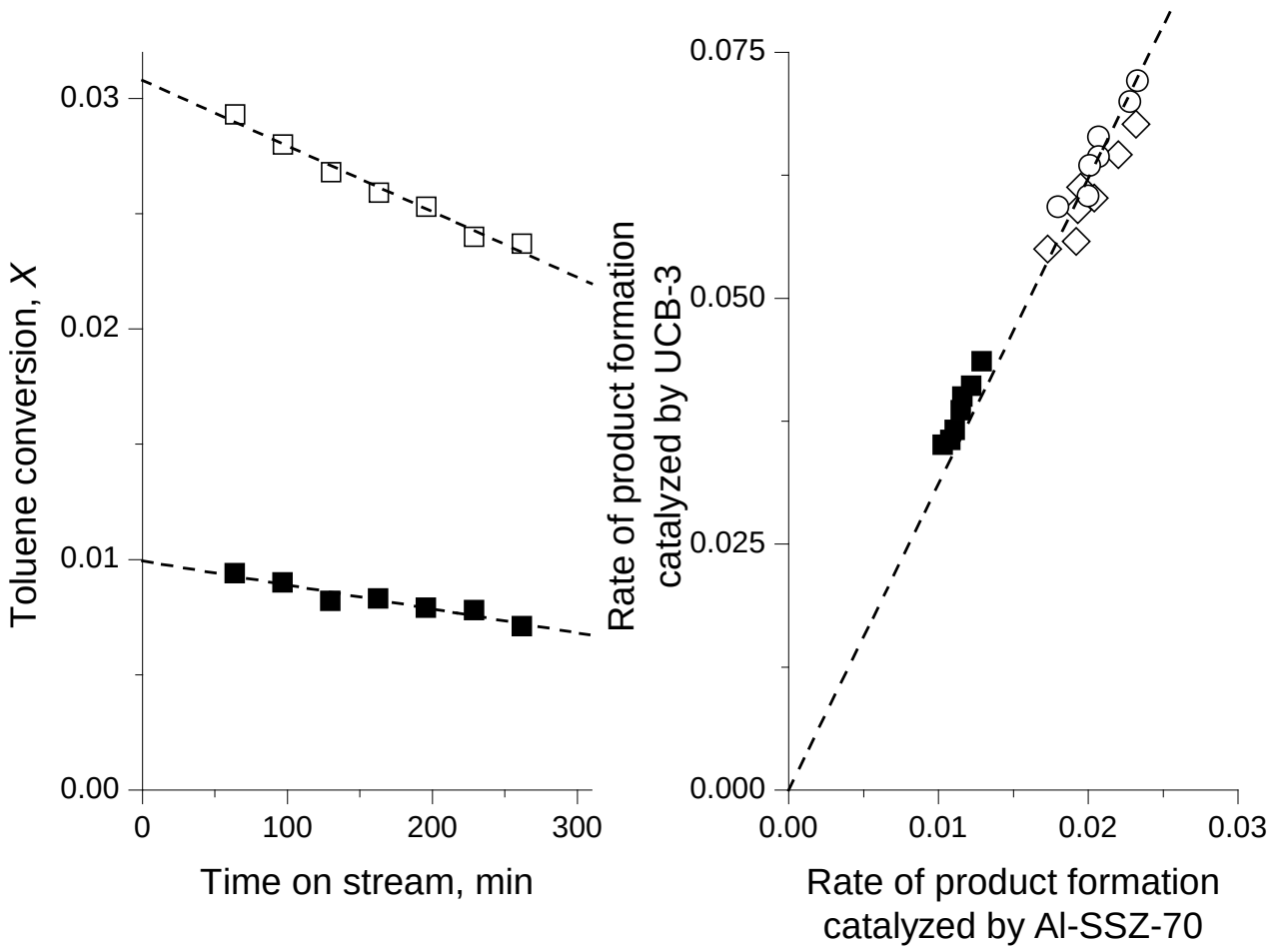

Figure S7. Change in toluene conversion catalyzed by UCB-3 (□) and Al-SSZ-70 (■) as a function of time-on-stream at 473 K and at 140 kPa (A). Cross-plot of the rates of product formation catalyzed by UCB-3 and by Al-SSZ-70 at 473 K at various times-on-stream, including data characterizing *m*- (■), *p*- (◇), and *o*- (○) isopropyltoluene (B). Units are in mol (g of catalyst)$^{-1}$ h^{-1} The data fit a linear model with a slope of 3.1, which is greater than the 2.5-fold increase in external-surface area observed with UCB-3 relative to that of Al-SSZ-70.

4 Supporting Information Tables

Table S1. Selectivities to cymenes versus time on stream in the alkylation of toluene with propylene catalyzed by calcined Al-SSZ-70, UCB-3, and Al-MCM-22 at 140 kPa and 523 K. The toluene conversion was < 0.03, and the propylene conversion was < 0.3.

Time-on-stream, min	Selectivity to cymenes formed in the conversion catalyzed by Al-SSZ-70			Selectivity to cymenes formed in the conversion catalyzed by UCB-3			Selectivity to cymenes formed in the conversion catalyzed by Al-MCM-22		
	m-	*p*-	*o*-	*m*-	*p*-	*o*-	*m*-	*p*-	*o*-
64	0.0197	0.0331	0.0243	0.0550	0.0767	0.0553	0.0247	0.0247	0.0339
97	0.0178	0.0305	0.0236	0.0524	0.0686	0.0495	0.0229	0.0229	0.0320
129	0.0169	0.0294	0.0220	0.0498	0.0701	0.0508	0.0204	0.0204	0.0288
162	0.0162	0.0259	0.0201	0.0495	0.0689	0.0507	0.0209	0.0209	0.0299
195	0.0157	0.0276	0.0216	0.0478	0.0654	0.0474	0.0197	0.0197	0.0285
228	0.0154	0.0260	0.0197	0.0467	0.0637	0.0468	0.0183	0.0183	0.0275

Table S2. Material characterization and catalysis data for Al-SSZ-70, silanated Al-SSZ-70, MCM-22 and silanated MCM-22. All materials have a Si:Al of 25, as determined by elemental analysis.

zeolite	microporosity[1] (cm^3/g)	reaction rate[2] at1 h TOS (mol toluene) (g of catalyst)$^{-1}$ h^{-1}
H-Al-SSZ-70	0.20	0.31
silanated H-Al-SSZ-70	0.19	0.13
H-Al-MCM-22	0.16	0.097
silanated H-Al-MCM-22	0.20	0.012

[1]t-plot method, thickness range 0.4-0.6 nm
[2]reaction temperature was 523 K.

5 References

(1) Archer, R. H.; Carpenter, J. R.; Hwang, S.-J.; Burton, A. W.; Chen, C.-Y.; Zones, S. I.; Davis, M. E. *Chem. Mater.* **2010**, *22*, 2563-2572.
(2) Ogino, I.; Eilertsen, E. A.; Hwang, S.-J.; Rea, T.; Xie, D.; Ouyang, X.; Zones, S. I.; Katz, A. *Chem. Mater.* **2013**, *25*, 1502-1509.
(3) Ding, W.; Meitzner, G. D.; Iglesia, E. *J. Catal.* **2002**, *206*, 14-22.
(4) Butt, J. B. *Reaction Kinetics and Reactor Design*; 2nd ed.; Marcel Dekker, Inc: New York, 2000, pp 254-255.
(5) Corma, A.; Martínez-Soria, V.; Schnoeveld, E. *J. Catal.* **2000**, *192*, 163-173.
(6) Ogino, I.; Eilersten, E. A.; Hwang, S.-J.; Rea, T.; Xie, D.; Ouyang, X.; Zones, S. I.; Katz, A. *Chem. Mater.* **2013**, *25*, 1502-1509..
(7) Ogino, I.; Nigra, M. M.; Hwang, S.-J.; Ha, J.-M.; Rea, T.; Zones, S. I.; Katz, A. *J. Am. Chem. Soc.* **2011**, *133*, 3288-3291.
(8) Roth, W. J.; Dorset, D. L. *Microporous Mesoporous Mater.* **2011**, *142*, 32-36.
(9) Kennedy, G. J.; Lawton, S. L.; Fung, A. S.; Rubin, M. K.; Steuernagel, S. *Catal. Today* **1999**, *49*, 385-399.
(10) Inagaki, S.; Kamino, K.; Kikuchi, E.; Matsukata, M. *Appl. Catal., A* **2007**, *318*, 22-27.
(11) Corma, A.; Diaz, U.; Fornés, V.; Guil, J. M.; Martínez-Triguero, J.; Creyghton, E. J. *J. Catal.* **2000**, *191*, 218-224.